Metalurgi (2017) 2: 53 - 66

METALURGI

Available online at www.ejurnalmaterialmetalurgi.com

FATIGUE FAILURE OF WHEEL STUDS AND NUTS OF LIGHT VEHICLES USED IN COAL MINE OPERATION

D.N. Adnyana
Department of Mechanical Engineering, Faculty of Industrial Technology
National Institute of Science and Technology (ISTN)
Jl. Moh Kahfi II, Jagakarsa, Jakarta Selatan 12640
E-mail: adnyanadn@yahoo.com

Masuk Tanggal :06-06-2017, revisi tanggal : 17-08-2017, diterima untuk diterbitkan tanggal 30-09-2017

Intisari

Kendaraan ringan merupakan moda transportasi yang potensial dan efisien digunakan dalam mendukung operasi tambang batubara. Akan tetapi, karena kondisi jalan yang sangat buruk pada lokasi pertambangan, banyak kendaraan ringan yang saat ini digunakan sering mengalami kecelakaan akibat terjadi kelonggaran pada roda. Terjadinya kelonggaran pada roda tersebut sangat terkait dengan patahnya atau rusaknya baut dan/atau mur roda kendaraan tersebut. Dalam makalah ini dibahas jenis kerusakan dan faktor-faktor yang kemungkinan telah menyebabkan terjadinya kerusakan pada baut dan/atau mur roda kendaraan. Penelitian/pengujian metalurgi telah dilakukan dengan menggunakan sejumlah benda uji yang diambil dari baut dan mur roda kendaraan, baik yang telah rusak maupun yang tidak rusak. Berbagai pengujian laboratorium telah dilakukan meliputi: uji makro, analisa komposisi kimia, uji metalografi, uji kekerasan dan uji SEM *(scanning electron microscopy)* yang dilengkapi dengan analisis EDS *(energy dispersive spectroscopy)*. Disamping itu, uji torsi juga telah dilakukan pada beberapa baut dan mur yang baru untuk mengukur hubungan antara momen torsi dan sudut torsi. Hasil dari penelitian/pengujian metalurgi yang diperoleh menunjukkan bahwa kerusakan pada baut roda disebabkan oleh retak atau patah lelah atau fatik akibat beban siklus yang bersifat tekukan searah dan pada tegangan nominal yang rendah.

***Kata Kunci**: Kendaraan ringan, baut dan mur roda, penelitian/pengujian metalurgi, retak atau patah fatik*

Abstract

Light vehicle is a potentially useful and efficient mode of transportation to be utilized in supporting the coal mine operation. However, due to the harsh road condition at the mine site, many light vehicles presently used are frequently experiencing a number of incidents caused by loose wheel. The occurrence of this loose wheel is very much related with some broken or damaged wheel studs and/or nuts of the vehicle. Type of failure and factors that may have caused the damage of the wheel studs and/or nuts of the vehicles are discussed in this paper. The metallurgical assessment was conducted by preparing a number of specimens from the damaged and undamaged wheel studs and nuts of the vehicles. Various laboratory examinations were performed including macroscopic examination, chemical composition analysis, metallographic examination, hardness test and SEM (scanning electron microscopy) examination equipped with EDS (energy dispersive spectroscopy) analysis. In addition, torsion test was also conducted on several new studs and nuts to measure the relationship between the torque and angular displacement. Results of the metallurgical assessment obtained show that the damaged wheel studs have experienced fatigue crack or fracture that was caused by load cycling under unidirectional bending at a low nominal stress.

***Keywords**: Light vehicle, wheel studs and nuts, metallurgical assessment, fatigue crack or fracture*

1. INTRODUCTION

A coal mine company utilizes a number of light vehicles (LV) to support its coal mine operation at several locations in East Kalimantan. Among of the light vehicles are presently used including the well-known brand name LV 4x4. According to the mine site information, the light vehicles presently used have been frequently experiencing a number of incidents caused by loose wheel. The occurrence of this loose wheel was very much related with some broken or damaged wheel studs and/or nuts of the vehicle.

A number of damaged and undamaged wheel studs and nuts of the light vehicles were received and used as representative of failure cases occurred on the mine site for metallurgical assessment. Studs A as shown in Figure 1(a) consist of one broken wheel stud and one undamaged wheel stud recovered from the front left hand wheel of the light vehicle after it had traveled 44675 km prior to the incident. Studs and nuts B as shown in Figure 1(b) consist of two bent studs, one undamaged stud, one damaged nut and one undamaged nut recovered from the other but the same brand name light vehicle as studs A obtained. These studs and nuts B were recovered from the front left hand wheel of the vehicle after it had traveled 46611 km before the incident occurred. In addition, there were also some new wheel studs and nuts selected and used for comparison in this investigation, namely studs C to represent a non OEM (original equipment manufacturer), see Figure 1(c), and studs D to represent the OEM of the same brand name of light vehicle as studs A and studs/nuts B obtained, see Figure 1(d).

The wheel stud material is generally specified as chromium steel, mainly used for machine structural application, manufactured by hot forming such as hot rolling or forging and followed by machining and heat-treatment. Under this condition, the wheel stud material is expected to achieve its maximum fatigue strength[1]. In addition, surface treatment such as case hardening is also frequently applied to the wheel stud for further increase on its surface hardness and strength against any fatigue cracking[2].

For the nut material, there are many possible materials available, but its requirement is that the nut material should have a lower hardness or strength in comparison with the stud material[2]. It is also frequently found that a nut can be made not only by one single material, but by two different materials. First part of the nut is a hollow body having with internal screw or thread which is usually made using a softer material compared to that used for the stud. The second part of a nut is its top cover which is usually joined to the hollow body by welding.

The purpose of this metallurgical assessment is to verify the material properties and determine whether the material used for the wheel stud and nut of the light vehicle met the specification or suitable for its operating condition. Furthermore, this assessment is also aimed to establish the type, cause and mode of failure of the damaged stud and nut of the light vehicles used, and based on the determination some corrective or remedial action may be initiated that will prevent similar failure in the future.

Figure 1. The as received damaged and undamaged wheel studs and nuts for metallurgical assessment. (a) Studs A recovered from the well-known brand name LV 4x4; (b) Studs and nuts B also recovered from the same brand name LV as studs A, but from different vehicle; (c) Studs C represent a non OEM; and (d) Studs D represent the OEM of the same brand name LV as studs A and studs B

2. MATERIALS AND METHOD

In performing this metallurgical assessment, a number of damaged and undamaged wheel studs and nuts of A, B, C and D shown in Figure 1 are used and a number of specimens were prepared for laboratory examinations. Macroscopic examination on surface damage of the wheel studs and nuts was performed using a stereo microscope, whereas chemical analysis was carried out using an optical spark emission spectrometer. The purpose of this chemical analysis is to determine whether the material used for the wheel studs and nuts met the specification or not. Metallographic examinations were also performed using an optical light microscope at various magnifications. The metallographic specimens were mounted using epoxy and prepared by grinding, polishing and etching. The etchant used was 5% Nital solution. A hardness survey was also carried out on the same specimens for the metallographic examination using Vickers hardness method at a load of 3kg (HV 3). Moreover, examination on some surface fracture of the damaged wheel stud was also performed using a SEM (scanning electron microscope) to determine the surface damage topography and nature of the failure. This SEM examination was also equipped with an EDS (energy dispersive spectroscopy) analysis to detect the presence of any manufacturing defect or corrosion by-product. In addition, torsion test was also conducted on several new studs and nuts on a test bench equipped with a load cell or sensor by stretching the stud during tightening of nut using a torque-meter. This test could measure the relationship between the torque and angular displacement on the stud. Maximum allowable preload torque could be noted or indicated as the stud may have been subjected to some plastic deformation (or permanent elongation), and at this condition the stud may suffer from loss of its preload.

3. RESULTS AND DISCUSSION

A. Macroscopic Examination on Fracture Surface of the Broken Stud

The fracture surface of the broken stud A is shown in Figure 2. It is clearly seen in this figure that the fracture occurs in the first thread of the stud and its fracture surface shows typical fatigue fracture having three distinctive areas of fracture, namely crack initiation, crack propagation and final fracture[3]. The fracture surface shown in Figure 2 also provides road signs of a unidirectional bending fatigue fracture with the initiation site located on an area having with a high stress concentration at the first stud-thread root immediately adjacent to the edge of the nut on the washer side. This stress concentration site occurs because the stud elongates as the nut is tightened, thereby producing increased loads on the threads nearest the bearing face of the nut, which add to normal service stresses[4]. The fatigue crack was then propagated along the stud cross section by forming beach marks as indicated in fracture surface in Figure 2. Shortly after the crack reached the other outer edge of the stud, a fast crack grew rapidly through the remaining section. The rough surface left by the fast crack is the final fracture. It can be seen from the fatigue fracture surface shown in Figure 2 that the final fracture zone is much smaller than the crack propagation (beach marks) area. This suggested that the fatigue fracture pattern of the broken stud shown in Figure 2 was produced by a low nominal stress. This is in accordance with the comparison shown in Figure 3, showing the schematic of marks on surface of fatigue fractures produced in smooth and notch components with round cross section under various loading conditions at high and low nominal stress[5].

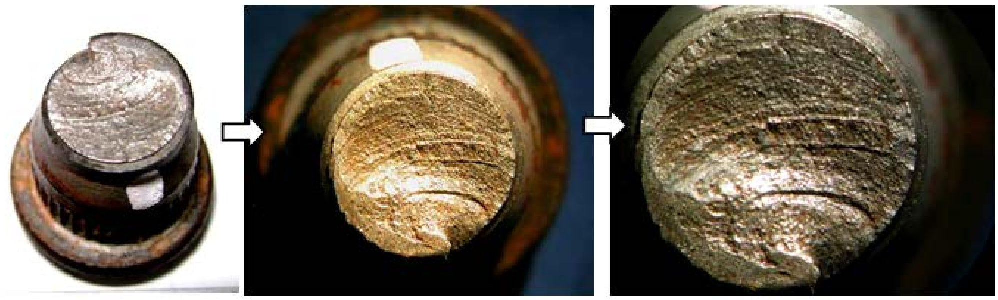

Figure 2. Fracture surface obtained from the broken wheel stud A

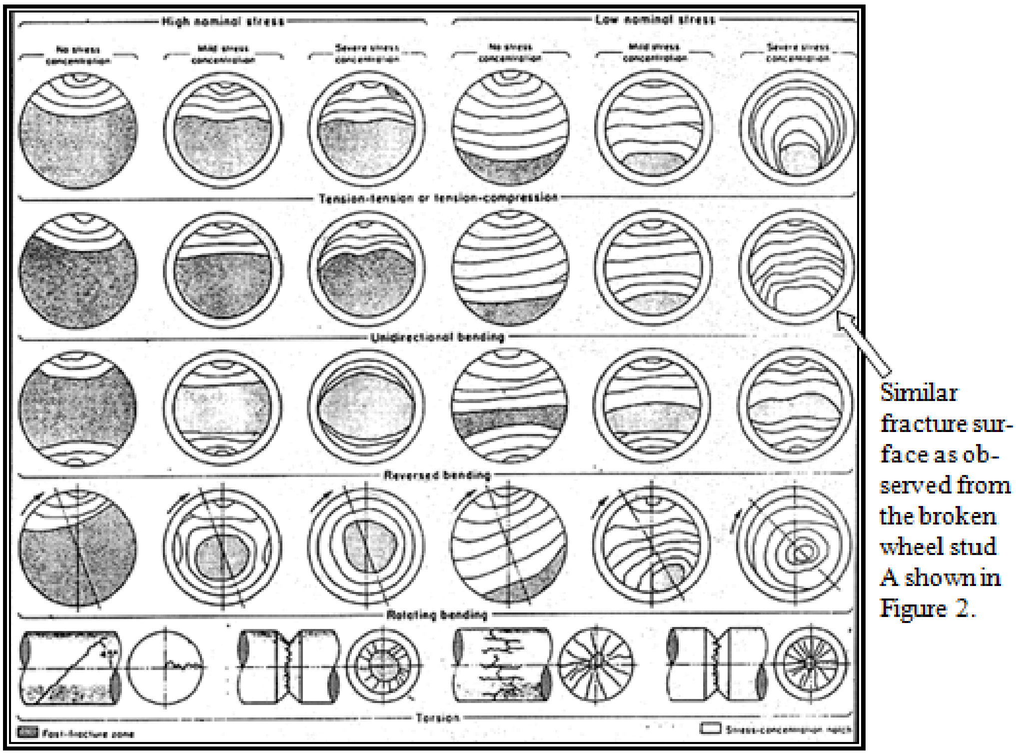

Figure 3. Schematic of marks on surfaces of fatigue fractures produced in smooth and notched components with round cross section under various loading conditions at high and low nominal stress[5]

B. Chemical Composition Analysis

The results of chemical analysis obtained from the damaged stud B, the new non OEM stud C and the new OEM stud D are presented in Table 1 in comparison with the standard materials. It can be seen from Table 1 that the chemical compositions of all the stud materials are approximately close and met to the material specification of JIS SCr415[6] and/or SAE/AISI 5120[7]. From Table 1, it can also be seen that the top cover of the damaged nut B is made of low carbon steel, different to that made for the nut hollow body.

Table 1. Results of chemical analysis obtained from the wheel studs and nuts of light vehicles in comparison with the standard materials

Element	Composition, wt.%					
	Damaged Nut (B2)	Deformed Stud (B1)	Non OEM New Stud (C1)	OEM New Stud (D1)	Standard Material	
					JIS SCr 415	SAE/AISI 5120
Fe	99.570	97.460	97.38	97.500	Balance	Balance
C	0.030	0.172	0.156	0.161	0.13 – 0.18	0.17 – 0.23
Si	0.008	0.211	0.189	0.207	0.15 – 0.35	0.40 max
Mn	0.280	0.738	0.789	0.729	0.60 – 0.85	0.60 – 0.90
S	0.008	0.006	0.006	0.009	0.030 max	0.020 – 0.035
P	0.016	0.017	0.008	0.010	0.030 max	0.035 max
Cr	0.026	1.087	1.117	1.088	0.90 – 1.20	0.90 – 1.20
Ni	0.020	0.071	0.076	0.074	-	-
Mo	0.002	0.023	0.028	0.019	-	-
Cu	0.017	0.167	0.183	0.148	-	-
Al	0.020	0.037	0.044	0.039	-	-
Ti	0.001	0.003	0.002	0.002	-	-
Nb	0.002	0.002	0.004	0.002	-	-

C. Results of Metallographic Examination and Hardness Test

Two polished and etched specimens of the longitudinal cross section of stud A are shown in Figures 4 and 5, which include the broken wheel stud and the undamaged wheel stud, respectively. Most of the microstructures obtained (see Figures 4 and 5) exhibit fine tempered martensite. This indicates that the wheel studs A were manufactured by rolling or forging, and then followed by a quench hardening and tempering heat-treatment. From the microstructures shown in Figures 4 and 5, no any significant manufacturing defect is observed in most area being examined of the wheel studs A. As also seen in Figures 4 and 5, some case hardening layer is also applied to the wheel studs A during their past manufacturing process. The application of this case hardening layer has increased the hardness of the stud skin material quite significantly in comparison with the stud core material. From Table 2, it can be seen that the hardness value in the range of 305-315 HV is obtained in most of the case hardening layer of the broken stud A, and this hardness range is higher than the hardness value of the stud core material which is only in the range of 269-276 HV. Similarly, the hardness value of the undamaged wheel stud A shown in Table 3 particularly on its thread surfaces is generally high in the range of 320 HV up to 420 HV, while the stud core material generally has a relatively lower hardness value in the range of 266 to 276 HV.

Table 2. Hardness value of studs A at different area

HV		
Area I	**Area II**	**Area III**
305	315	276
276	310	269

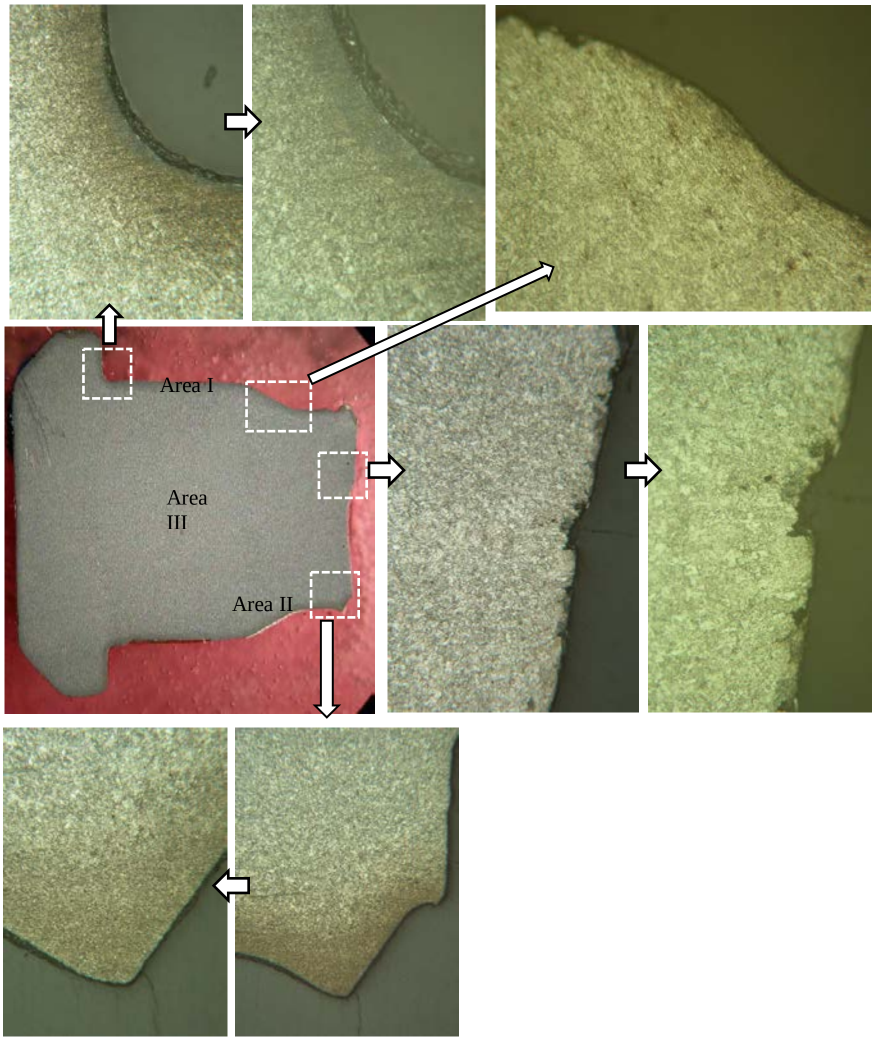

Figure 4. Microstructures obtained from the broken wheel stud A at different locations, showing fine tempered martensite. Etched with 5% Nital solution

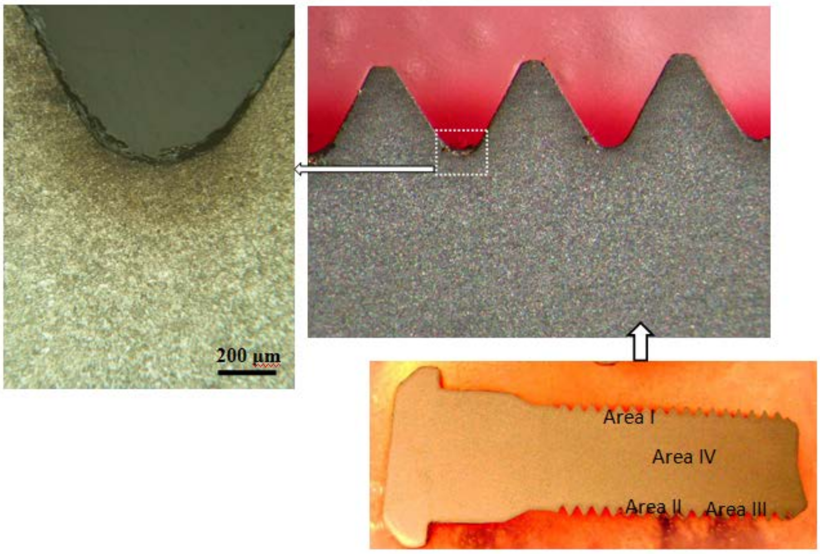

Figure 5. Microstructures obtained from the undamaged wheel stud A at location as indicated by the square grit, showing fine tempered martensite. Etched with 5% Nital solution

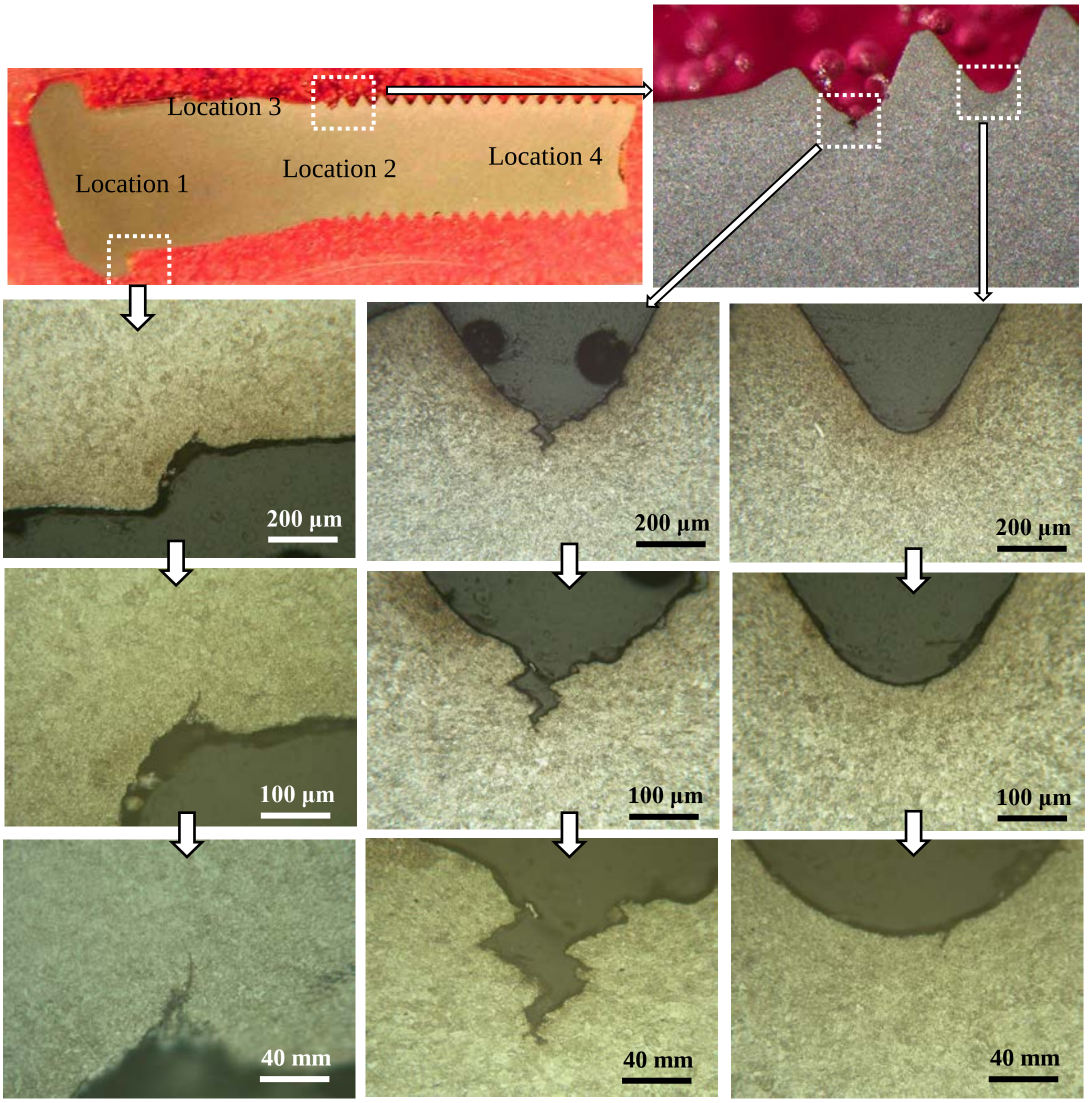

Figure 6. Microstructures obtained from the damaged (bent) wheel stud B at locations as indicated by the square grit, showing fine tempered martensite. Etched with 5% Nital solution

Table 3. Hardness value of the undamaged wheel stud A at different area

HV			
Area I	**Area II**	**Area III**	**Area IV**
412	420	386	276
399	412	325	266
380	392		
	320		

Table 4. Hardness value obtained from the damaged (bent) wheel stud B at different locations

HV			
Location 1	**Location 2**	**Location 3**	**Location 4**
242	191	218	126
256	187	225	135
218	164	215	141

Table 5. Hardness value obtained from the damaged nut B at different locations.

HV					
Location 1	**Location 2**	**Location 3**	**Location 4**	**Location 5**	**Location 6**
105	128	252	294	292	245
102	135	246	288	294	210
		248	248	251	165

Similar to studs A, the microstructures obtained from studs B also generally exhibit fine tempered martensite, see Figure 6. It is also seen in Figure 6 that a fatigue crack may have been initiating at the first thread root of the bent stud B. In addition, a fine fatigue crack due to bending may have also been developing at the root of its second thread. Furthermore, other fine fatigue crack may have also been initiating from a high stress concentration area at the head-to-shank fillet of the stud (see Figure 6). Moreover, there is no any manufacturing defect observed in most of the fatigue crack area formed in the wheel stud B. Although the microstructures obtained from the wheel studs B are very much similar with that obtained from the wheel studs A, however, the average hardness value of the damaged stud B is relatively lower compared to the average hardness value of the studs A (see Table 4). This difference in hardness may be associated with the difference in the parameters applied during the manufacturing process for the wheel studs B and A. It is also likely that the stud B has not been given with sufficient case hardening layer.

For the damaged nut B, the microstructures obtained are shown in Figure 7. It is clearly seen that the damaged nut B is made of two parts, a hollow part having some internal screws or threads, and a top cover that was joined to the hollow part by welding. Microstructures of the top cover part consist of a predominant ferrite with some small amount of pearlite, typical of a low carbon steel material. This is supported by the hardness test results shown in Table 5 in which its hardness value is relatively low (in the range of 102-135 HV). On the other hand, the microstructures of the hollow part of the nut B shown in Figure 7 contain higher amount of pearlite in the ferrite matrix. This indicates that the hollow part of the nut B was made from carbon steel containing higher carbon compared to the top cover material of the nut B. The average hardness value of the hollow part of the nut B is also much higher compared to the average hardness value of the top cover material of the nut B, especially in the area around the internal screws or threads (see Table 5). However, in contrary this high hardness of the internal threads of the nut B is higher than the hardness of the stud threads of stud B. It can also be seen from Figure 7 that most of the nut B's external surface has been given with some coating of about 50 μm in thickness. The coating applied is most likely typical of hard chrome plating.

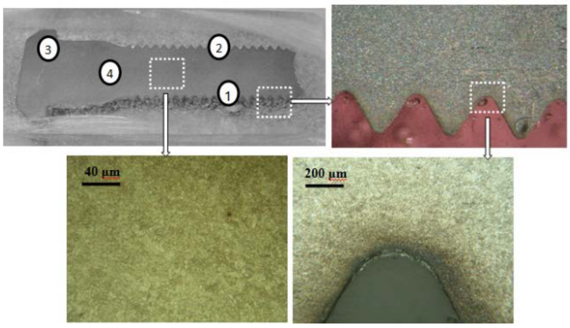

Figure 8. Microstructures obtained from the brand new non-OEM wheel stud C at locations as indicated by the square grit, showing fine tempered martensite. Etched with 5% Nital solution

Most of the microstructures obtained from the non-OEM wheel stud C (see Figure 8) also exhibit fine tempered martensite, similar to the microstructures obtained from the wheel studs A and B. It is also seen from the microstructures that a case hardening is also applied on most of the stud C surfaces. As seen in Table 6, the hardness value of the stud C surface is found in the range of 352 to 441 HV, much higher than the hardness value of its core material which is in the range of 320 to 325 HV. The associated wheel nut C together with its ring washer is also examined, and its microstructures obtained are presented in Figure 9. It is clearly seen that the entire wheel nut C is made from the same material of a low carbon steel in which its microstructures consisting of a small amount of pearlite in the predominant soft and ductile ferrite matrix. It can also be seen that there is likely not any coating applied to the external surface of the wheel nut C.

Table 6. Hardness value obtained from the brand new non-OEM wheel stud C at different locations

HV			
Location 1	**Location 2**	**Location 3**	**Location 4**
402	441	325	320
375	356	344	325
352	-	352	325

For wheel stud D, its microstructures consist of fine tempered martensite, similar to those obtained from the wheel studs A, B and C (see Figure 10). It can also be seen that a case hardening layer may have also been applied to the wheel stud D. The hardness value obtained from the stud D thread surface is in the range of 330 to 495 HV, while the hardness value obtained from its stud core material is in the range of 283 to 306 HV (see Table 7). This hardness value of the core material of the stud D in average is relatively lower than the hardness value of the core material of stud C, but the stud D has the average surface hardness higher than the average surface hardness of stud C.

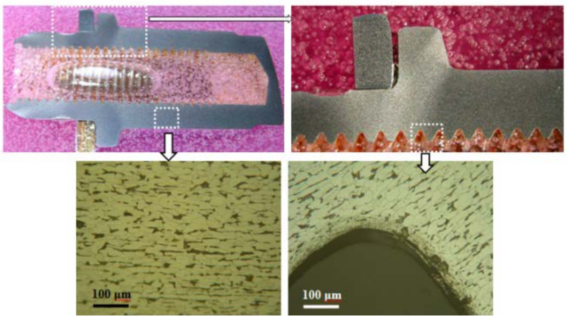

Figure 9. Microstructures obtained from the brand new non-OEM nut C at locations as indicated by the square grit, showing ferrite matrix with some small amount of second phase of pearlite. Etched with 5% Nital solution

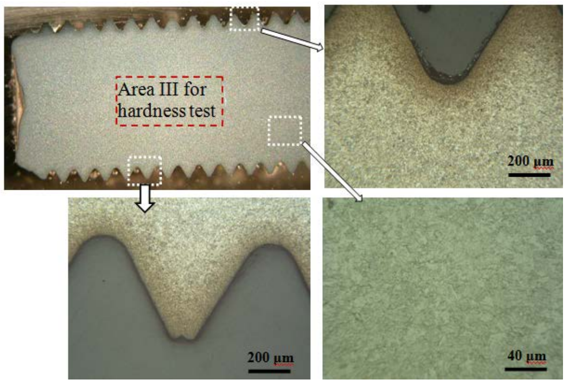

Figure 10. Microstructures obtained from the brand new OEM wheel stud D at locations as indicated by the square grit, showing fine tempered martensite. Etched with 5% Nital solution

Table 7. Hardness value obtained from the brand new OEM wheel stud D at different area

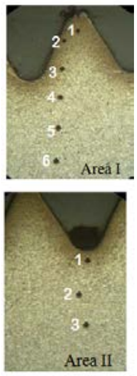

No	Hardness Value (HV) Area I	Area II	Area III
1	495	444	283
2	480	402	285
3	356	301	
4	330	298	
5	306		
6	285		

D. SEM Fractography and EDS Analysis

The SEM fractographs of the surface fatigue fracture of the broken wheel stud A are presented in Figure 11. It can be seen that some of the fracture surfaces of the broken stud material exhibit less distinct striations of typical fatigue appearance of low alloy steel[8]. Although fatigue striations are not well resolvable at any location, but the entire fatigue fracture surface displays similar crystallographic features. Further evidence of the occurrence of fatigue fracture is also indicated by the fact that no any plastic deformation in the form of dimple fracture is observed on most of the SEM fractographs shown in Figure 11[2].

The EDS spectrum obtained from the fatigue fracture surface of the broken wheel stud A at some test location is presented in Figure 12. The EDS spectrum show some major elements of the low-alloy steel containing chromium from which the wheel stud A was made such as: Fe, C, Si, Cr, Al and Mo. In addition, some other elements are also present such as: O, F, Zn, K and Ca. Oxygen (O) is likely coming from the oxide scale that may be present on the fracture surface of the wheel stud material, whereas Zn is most likely coming from the zinc coating that may have been applied to the stud surface. The source of F, K and Ca is not clearly known, but they may be coming from the road soil and/or from the environment. However, the presence of these elements in small amounts may have not significantly affected to the stud damage as there is no any corrosion by product is observed to form on most of the fracture surface of the broken stud A.

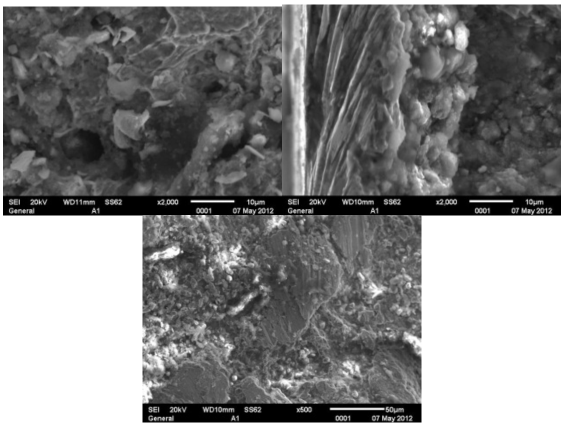

Figure 11. SEM micrographs obtained from the surface fatigue fracture of the broken wheel stud A

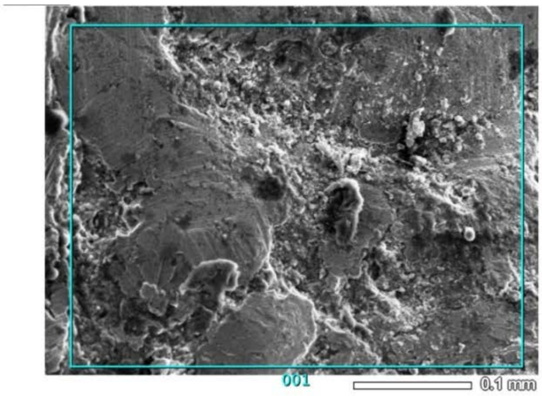

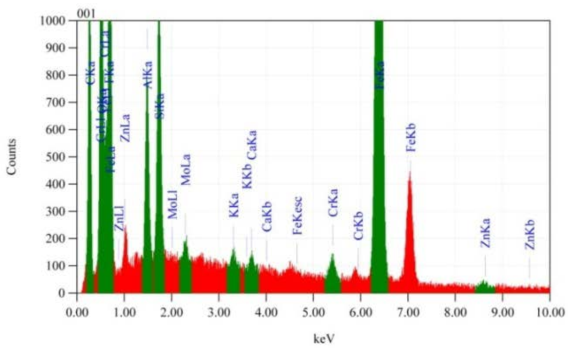

ZAF Method Standardless Quantitative Analysis
Fitting Coefficient : 0.2845

Element	(keV)	Mass%	Error%	Atom%	Compound	Mass%	Cation	K
C K	0.277	24.33	0.12	45.01				7.8601
O K	0.525	20.19	0.23	28.04				22.3199
F K	0.677	2.82	0.22	3.30				1.1627
Al K	1.486	3.07	0.14	2.53				2.3103
Si K	1.739	3.75	0.13	2.96				3.5266
K K*	3.312	0.23	0.13	0.13				0.3561
Ca K*	3.690	0.28	0.14	0.15				0.4522
Cr K	5.411	0.68	0.22	0.29				1.0706
Fe K	6.398	43.16	0.32	17.17				59.2010
Zn K	8.630	0.62	0.89	0.21				0.7801
Mo L*	2.293	0.87	0.29	0.20				0.9605
Total		100.00		100.00				

Figure 12. EDS spectrum of elements representing the corresponding composition of fracture surface of the broken wheel stud A

E. Factors Affecting Fatigue Failure on the Wheel Studs or Nuts

The occurrence of loose wheel on the vehicle during its operation is very much dependent on the rigidity of the wheel-hub joint of the vehicle, and this is influenced by the degree of preload applied to the stud [9]. As the working load is applied during operation, the preloaded stud does not encounter any additional load until the working load equals to the stud preload. When the applied working load exceeds over the stud preload, the stud starts to lose its preload and its associated clamping force as well. With a fluctuating load during operation, this situation can cycle the stud progressively, with continued loss of preload and possible rapid fatigue failure. To eliminate fatigue problem that may occur on the wheel stud, it is usually considered to specify as high an initial preload as practical.

There are four possible factors that may have contributed to the acceleration of fatigue failure occurred on the wheel studs and/or nuts of the light vehicles operated at the harsh road condition of the coal mine site, either singly or in combination.

The four possible factors are given as follows:

(i). Improper use of the vehicle

This means that the vehicle has not been operated properly in such harsh road condition at the mine site so that the stud-wheel joint of the vehicle is subjected to an excessive or severe working load. As schematically illustrated in Figure 13, this severe working load when exceeded the stud preload, it could start to reduce the clamping force between the stud and the wheel joint and hence could establish a highly dynamic cyclic load condition. With the high fluctuating load due to road condition, this situation could cycle the wheel stud progressively, with continued loss of preload and thus resulted in a loose joint, and eventually followed by a possible rapid fatigue failure.

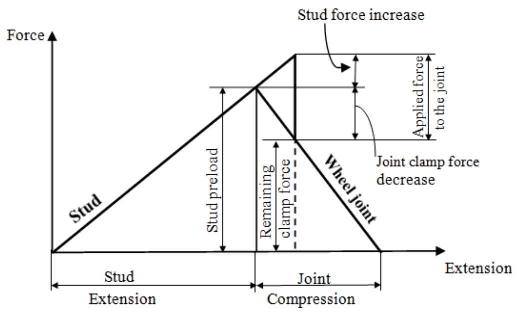

Figure 13. Diagram force versus extension of stud-wheel joint under an applied external force

(ii). Improper material of the stud

The yield and tensile strength of the studs A or B (see Figure 14 for the stud material X) may not be sufficient to withstand for the severe working load occurred on the harsh road condition at mine site. As a result, the studs A or B which is made from the material X was likely not able to accommodate a high (initial) preload during its installation if compared to a stud that made of material Y (see Figure 14). It can be seen from Figure 14 that material Y has higher yield and tensile strength than this material X. In practice, a high initial preload is actually required to obtain a high clamping force that make more rigid joint and thus increase stud fatigue life. Due to this limitation, the preload that could be applied to the stud A or B became relative low, and therefore the clamping force of joint tended to decrease easily when subjected to a severe load condition and thus resulted in a loose joint and eventually followed by a rapid fatigue crack or fracture.

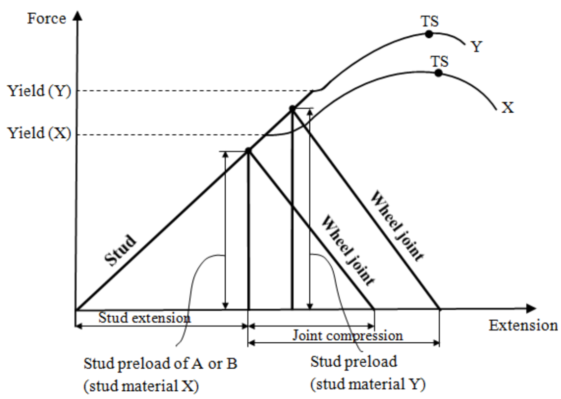

Note:
Yield or tensile strength (TS) of material Y > Yield or tensile strength (TS) of material X

Figure 14. Diagram of stud-wheel joint having two different preloads due to the difference in stud material used

(iii). Improper material of the wheel

The wheel material of light vehicle presently used is generally made using some aluminum alloy. The application of this aluminum wheel could result a “soft” joint (a high stiffness stud with a low stiffness joint), because the stiffness slope of the wheel stud is greater than that of the wheel joint and could result in a low preload (see Figure 15)[10]. As seen in Figure 15, when using a steel wheel it could result in a “hard” joint (a low stiffness stud with a high stiffness joint) and provides a higher initial preload compared to the aluminum wheel. The steel wheel joint could be subjected to a high working load compared to the aluminum wheel joint and therefore the clamping force of steel wheel joint could maintain its stability/rigidity. As seen in Figure 15, for the same applied force to the wheel joint, the stud would sustain the majority of the applied force when the wheel material is made of aluminum compared if the wheel material is made of steel. Consequently, under a severe load condition the clamping force of Al wheel joint could decrease rapidly and establish a highly dynamic cyclic loading condition, leading to a rapid fatigue on the stud.

(iv). Incorrect installation of the stud and wheel joint

If the wheel and its hub are not secured snugly by the studs due to insufficient tightening of the studs, the resulting preload becomes low, and the working load is the imminent likelihood to exceed the stud preload and could reduce the clamping force (see Figure 16). Consequently, a slight movement of the wheel relative to the studs could generate some dynamic cyclic loads and could initiate fatigue cracking.

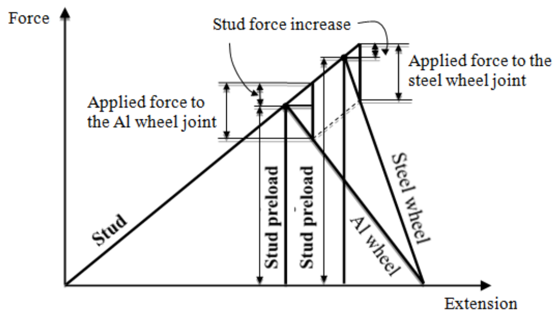

Figure 15. Diagram of stud-wheel joint having two different wheel materials, one is made of aluminum alloy and the other is made of steel

Each time the wheel made one revolution, unidirectional bending would occur on the studs. After fatigue started, the loosening of any stud would increase the stress on the remaining studs until they all failed. On the other hand, when the studs were over torqued, the stretch occurred on the studs could exceed the elastic limit, and the stud experienced some plastic deformation, taking a permanent set (see Figure 16). This typical damage due to some plastic deformation may have occurred on the studs B. This could result a loss in stud preload, and the clamping force acting on the wheel and hub joint would continue to decrease. Under high fluctuating loads during operation due to a severe road condition, this situation could cycle the stud progressively with continued loss of preload and possibly rapid fatigue failure. In addition, over torqueing would also cause the nut-thread stripping that may have also contributed to rapid stud failure.

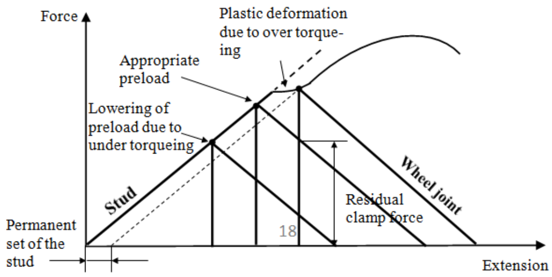

Figure 16. Diagram of stud-wheel joint under different preloads due to the difference in torques applied

Some of the test results of torque and angular displacement measurement obtained from the wheel stud/nut joint of studs D (OEM new stud/nut) and studs C (non-OEM new stud/nut) are presented in Figure 17. All of the test results obtained are then summarized and presented in Table 8. It can be seen from Table 8 that all studs D of the OEM wheel stud/nut could provide the torque at elastic limit higher than the non-OEM of studs C. On the other hand, the torque at maximum plastic limit of the OEM wheel stud/nut of studs D is relatively lower compared to the non-OEM wheel stud/nut C. The difference in torque versus angular displacement relationship between the OEM wheel stud/nut D and the non-OEM wheel stud/nut C might be associated with the difference in material used and/or by the difference in manufacturing process applied on both studs and nuts (see the chemical composition shown in Table 1 and the microstructures of studs D and C in Figures 8 and 10). Generally accepted that the wheel stud/nut having with higher torque at elastic limit is preferable being used for joint application. The higher the torque at elastic limit that the wheel stud/nut could withstand, the higher the preload that could be given to the joint. In practice, the highest initial preload is usually required by the joint in order to reduce its tendency of suffering from a possible loss in preload or clamping force during operation.

Furthermore, it can be seen from Table 8 that when the initial torque of 50 N-m is taken into account, then the maximum permissible torque that could be given to the OEM wheel stud/nut of studs D is in the range of 125 to 175 N-m or 12.74 to 17.83 kg-m, whereas for the non-OEM wheel stud/nut C, the maximum permissible torque that could be given is in the range of 90 to 140 N-m or 9.17 to 14.27 kg-m. According to the information obtained from a Car Dealer, stated that by experience, the preload torque is usually applied to the wheel stud/nut joint with a maximum torque of 11.50 kg-m, whereas in the manual book shows that the preload torque is recommended being 10.70 kg-m.

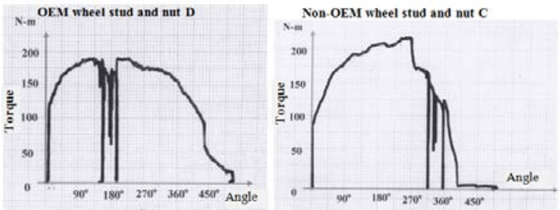

Figure 17. The torque and angular displacement curves obtained from the test of the wheel studs and nuts

Table 8. Results of torque and angular displacement measurement obtained from the OEM of stud D and the non-OEM of stud and nut C

Wheel stud/nut	Torque			
	Torque at Elastic Limit		Torque at Maximum Plastic Limit	
	N-m	kg-m	N-m	kg-m
OEM wheel stud and nut D1	150	15.28	165	16.82
OEM wheel stud and nut D2	125	12.74	190	19.37
OEM wheel stud and nut D3	140	14.27	212	21.61
Non-OEM wheel stud and nut C1	100	10.19	190	19.97
Non-OEM wheel stud and nut C2	90	9.17	230	23.44

4. CONCLUSIONS

The results of chemical analysis obtained show that the material used for all wheel studs under study such as the used and damaged studs A and B, and the unused or new studs C and D is very much close and met to the material specification of JIS G4104 Class SCr 415 and/or SAE/AISI 5120, a typical low alloy steel containing chromium that mainly used for machine structural application.

It is also found that all wheel stud materials under study exhibit similar microstructures of fine tempered martensite. This indicates that all the wheel studs were manufactured by hot forming such as hot rolling or forging and then followed by machining, quench hardening and tempering heat treatment.

Although all the wheel studs exhibit similar microstructures of fine tempered martensite, however the average hardness value of the stud core material A and D have similar hardness value in the range of 266 to 285 HV, or 24.8 to 27.8 HRC, whereas the stud core material C has the highest hardness value of 320-325 HV, or 32.2-32.5 HRC. On the other hand, the stud core material B shows the lowest hardness range of 126 to 191 HV, or 120 to 182 HB. The difference in this hardness value obtained among the stud material may be associated with the difference in parameters that may have been applied during the manufacturing process of the studs. In addition, all the wheel studs under study are also given with case hardening layer in order to further improve the surface strength of the studs against fatigue crack.

Most of the wheel nut material is made of low carbon steel having microstructure of ferrite as matrix phase and pearlite as second phase. In general, this wheel nut material is softer than the material of the stud, except for the wheel nut B in which its average hardness value is somewhat higher than the average hardness value of the stud. Due to its low hardness, it may have caused the stud B to become susceptible to plastic deformation.

According to the fracture topography and mode of failure, the broken stud A has experienced fatigue fracture that was caused by a load cycling under unidirectional bending at low nominal stress. Similar fatigue crack was also observed on the damaged wheel stud B. There is no any significant manufacturing defect or corrosion encountered around the fatigue crack area of the studs that may have contributed to initiate the fatigue crack.

There are four possible factors that may have contributed to the acceleration of fatigue failure on the wheel studs or nuts of the vehicles, either singly or in combination, including improper use of the vehicle, improper material of the wheel stud, improper material of the wheel, and/or incorrect installation of the stud and wheel joint.

From the results of torsion test obtained, it is found that the OEM studs D could accommodate higher maximum permissible torque than that of the non-OEM studs C. Maximum permissible torque that can be applied to the OEM stud D is in the range of 125 to 175 N-m, or 12.74 to 17.83 kg-m, whereas for the non-OEM stud C, the maximum permissible torque that can be applied is in the range of 90 to 140 N-m, or 9.17 to 14.27 kg-m.

ACKNOWLEDGEMENT

The author wishes to express his gratitude to the head and members of Department of Mechanical Engineering, Faculty of Industrial Technology of the National Institute of Science and Technology (ISTN) for their support and encouragement in publishing this work.

REFERENCE

[1] M. R. Hasan, "Failure Investigation Report on Different Components of an Automotive Engine", *International Journal of Mechanical Engineering and Applications*, vol. 5, no.1, pp. 47-51, 2017.

[2] "Failures of Mechanical Fasteners", Handbook: Failure Analysis and Prevention, *ASM International*, vol.11, pp. 531-541, 1998.

[3] R.J.Shipley, P.C.Bouldin, E.W.Holmes, "In-Service Failure of SAE Grade 8.1 Wheel Studs", Handbook of Case Histories in Failure Analysis, *ASM International*, vol. 2, pp. 73-75, 1993.

[4] S.N.Yadav, N.S.Hanamapure, "Analyze the Effect of Slip Angle on Fatigue Life of Wheel Rim of Passenger Car by Using Radial Fatigue Testing", *International Journal of Innovative Research in Science, Engineering and Technology*, vol. 2, pp. 4309-4318, September 2013.

[5] D.N.Adnyana, "Metallurgical Assessment of a Broken Gearbox Intermediate Shaft of a Reciprocating Compressor", *Metalurgi - Majalah Ilmu dan Teknologi*, vol. 31 (1), pp. 19-32, April 2016.

[6] "Ferrous Materials & Metallurgy I", Japanese Standards Association, JIS Handbook., pp. 1181-1182, 2001.

[7] "Guide to Engineered Materials 2002", Advanced Materials and Processes, pp. 58-60, December 2001.

[8] W.F.Jones, Fatigue Failure of a 1000 mm Diameter Trailer Wheel at the Bolt Holes, Handbook of Case Histories in

Failure Analysis, ASM International, vol. 1, pp. 85-87, 1992.
[9] C.W.Ferrone, D.Kopernik, “Heavy Truck Wheel Separation-Failure Modes and Classifications”, *Safety Brief*, vol. 13, pp. 1-6, December 1997.
[10] S.Das, “Design and Weight Optimization of Aluminum Alloy Wheel”, *International Journal of Scientific and Research Publication*, vol. 4, pp. 1-12, June 2014.